


Active phase separation: A universal approach

Fabian Bergmann, Lisa Rapp, and Walter Zimmermann*

Theoretische Physik I, Universität Bayreuth, 95440 Bayreuth, Germany (Received 31 January 2018; revised manuscript received 18 April 2018; published 24 August 2018)

We identify active phase separation as a generic demixing phenomenon in nonequilibrium systems with conservation constraints. Examples range from cell polarization to cell populations communicating via chemotaxis, and from self-propelled particle communities to mussels in ecology. We show that system-spanning properties of active phase separation in nonequilibrium systems near onset are described by the classical Cahn-Hilliard (CH) model. This result is rather surprising since the CH equation is famous as a model for phase separation at thermal equilibrium. We introduce a general reduction scheme to establish a unique mathematical link between the generic CH equation and system-specific models for active phase separation. This approach is exemplarily applied to a model for polarization of cells and a model for chemotactic cell communities. For cell polarization, we also estimate the validity range of the CH model.

DOI: [10.1103/PhysRevE.98.020603](https://doi.org/10.1103/PhysRevE.98.020603)

Demixing phenomena in active, nonequilibrium systems currently attract great attention. Examples include cell polarization [1–12], chemotactically communicating cells [13–17], self-propelled particles [18–21], active matter models [22], mixtures of particles with different mobilities [23–26], models of ion-channel densities [27], or mussels in ecology [28]. All of these examples have three properties in common: First, they resemble classic equilibrium phase separation. Second, in contrast to classic phase separation, these are nonequilibrium transitions. Third, they are all subject to conservation constraints. Since these demixing phenomena take place in nonequilibrium systems, we call them *active phase separation*. Their (local) driving mechanisms are as different as the systems themselves. But do these systems nevertheless share fundamental properties described by a generic model? Here we provide a universal framework for the cross-system characteristics of a class of active phase separation phenomena.

A conceptual parallel to this idea are self-organized patterns in nature. Stripe, hexagonal, or traveling wave patterns are driven by mechanisms that are also as diverse as the systems in which they form [29–34]. Nevertheless, periodic patterns in these different nonequilibrium systems share well-known generic properties [33,34]. They are covered by unconserved order-parameter fields that describe the slowly varying amplitude(s) [envelope(s)]. Even though stripe patterns occur in very different systems, the envelope obeys the same fundamental (nonlinear) Ginzburg-Landau equation [33,34]. It can be derived from basic equations and provides the key to understanding the generic properties of stripe patterns [30,34–36].

In this work, we formulate a similar approach for active phase separation in nonequilibrium systems. We present a reduction scheme generalized to conserved order parameters. At leading order, we thereby obtain the Cahn-Hilliard model [37,38] as the generic model for active phase separation

in nonequilibrium systems. So far, it has typically been used to model liquid-liquid demixing in thermal equilibrium [37,38]. However, we show here that it also describes the system-spanning properties of phase separation in nonequilibrium. Thus, we manage to capture the essence of active phase separation in very different systems in one universal equation. At the same time we expose the underlying similarities between phase separation in and out of equilibrium. The reduction scheme we present here provides a direct mathematical link between the Cahn-Hilliard (CH) model and system-specific models. It also provides the criteria to identify candidates for this class of active phase separation. Our approach is explicitly demonstrated for two representative examples from living matter: a continuum model for cell polarization and a model for chemotactic cell communities.

Cell polarization is central to processes as diverse as cell motility, differentiation, and cell division [1–10]. The polarized cell has two distinct regions similar to the two phases of a separated liquid-liquid mixture. However, cell polarization in living systems is a nonequilibrium phenomenon driven by *dissipative* processes. The molecules that trigger cell polarization are conserved on the timescales of the self-organization. Models for cell polarization usually involve the nonlinear dynamics of several coupled concentration fields for regulating molecules (see, e.g., [4]). However, minimal models with only two concentration fields for the membrane-cytosol exchange already cover essential properties [5–10]. One concentration field $\tilde{u}(\mathbf{r}, t)$ thereby represents molecules bound to the membrane. The other concentration field $\tilde{v}(\mathbf{r}, t)$ describes molecules in the cytosol. Here, we use

$$\tilde{f}(\tilde{u}, \tilde{v}) = -b\tilde{u} + (\tilde{u} + \tilde{v})^2 - (\tilde{u} + \tilde{v})^3 \quad (1)$$

for the membrane to cytosol exchange in the one-dimensional equations for the fields \tilde{u} and \tilde{v} :

$$\partial_t \tilde{u} = D_u \partial_x^2 \tilde{u} + \tilde{f}(\tilde{u}, \tilde{v}), \quad (2a)$$

$$\partial_t \tilde{v} = D_v \partial_x^2 \tilde{v} - \tilde{f}(\tilde{u}, \tilde{v}) \quad (\text{model } P). \quad (2b)$$

*Corresponding author: walter.zimmermann@uni-bayreuth.de

Both fields are coupled via the conservation condition

$$M = \frac{1}{L} \int_0^L [\tilde{u}(x) + \tilde{v}(x)] dx. \quad (3)$$

Another variant of a nonequilibrium phase separation process is clustering of chemotactically communicating cells. They play, for instance, a central role on the route to multicellular fruiting bodies [39]. Here the number of cells is conserved on the timescale of the clustering, but the chemical density field for the cell-cell communication is not [13–17]. We describe a system of chemotactically communicating cells by an extended Keller-Segel model [13–16] with cell density $\tilde{\rho}(\mathbf{r}, t)$ and signal molecule density $\tilde{c}(\mathbf{r}, t)$:

$$\partial_t \tilde{\rho} = \partial_x^2 \tilde{\rho} - s \partial_x \left(\frac{\tilde{\rho}}{1 + \beta \tilde{\rho}} \partial_x \tilde{c} \right), \quad (4a)$$

$$\partial_t \tilde{c} = D_c \partial_x^2 \tilde{c} + \tilde{\rho} - \tilde{c} \quad (\text{model } C). \quad (4b)$$

Model *P* in Eqs. (1) and model *C* in Eqs. (4) have spatially homogeneous solutions u_h, v_h or ρ_h, c_h , respectively. These become unstable beyond critical values of the respective control parameters D_v and s . Immediately above these thresholds, a generic equation can in both cases describe the resulting active phase separation. In the following steps we develop this equation for the conserved order-parameter field.

For both models, we separate the inhomogeneous parts from the basic state, writing $\tilde{u} = u_h + u(x, t)$, etc. We first consider the instability of the homogeneous states with respect to small perturbations. The linear equations in u, v are then solved by the ansatz $u, v = \tilde{u}, \tilde{v} \exp(\sigma t + i q x)$ (or for ρ and c , respectively). We consider the case when one of two eigenvalues $\sigma_{1,2}$ is always negative close to the onset of phase separation. The other eigenvalue, expanded with respect to powers of q^2 , is of the form

$$\sigma = G_2 q^2 - G_4 q^4 + O(q^6) \quad (5)$$

with $G_4 > 0$. The leading order coefficients $G_2^{(P)}$ or $G_2^{(C)}$ include the control parameters D_v and s for models *P* and *C*, respectively. The homogeneous solutions become linearly unstable for $G_2 > 0$. $G_2 = 0$ thus defines the critical values of the control parameters:

$$D_v^c = D_u f_v / f_u, \quad s_c = (\rho_0 h)^{-1}, \quad (6)$$

where $f_{u,v} = \partial_{u,v} f$ and $h = (1 + \beta \rho_0)^{-1}$. As a measure for the distance from the onset of phase separation, we choose the dimensionless control parameter ε , where

$$D_v = D_v^c (1 + \varepsilon), \quad s = s_c (1 + \varepsilon). \quad (7)$$

Next, we consider the basic equations [cf. Eqs. (2) and (4)] in the range of small ε , i.e., $G_2 \propto \varepsilon$. With $G_4 = O(1)$ the growth rate σ becomes positive in a range of small $q^2 \propto \varepsilon$ and is of the order $\sigma \propto \varepsilon^2$. Therefore, we introduce the “slow” spatial scale $X = \sqrt{\varepsilon} x$ and the timescale $T = \varepsilon^2 t$, which is slower than for periodic patterns [34]. The nonlinear analysis demands the introduction of an additional slow timescale, $T_3 = \varepsilon^{3/2} t$ [40]. This leads to the operator replacements

$$\partial_x \rightarrow \sqrt{\varepsilon} \partial_X, \quad \partial_t \rightarrow \varepsilon^{3/2} \partial_{T_3} + \varepsilon^2 \partial_T. \quad (8)$$

In compact matrix form, Eqs. (2) and (4) are

$$\partial_t \mathbf{w} = \mathcal{L} \mathbf{w} + \mathbf{N}, \quad (9)$$

with the respective vectors $\mathbf{w} = (u, v)$ and $\mathbf{w} = (\rho, c)$. The right-hand side includes a linear part $\mathcal{L} \mathbf{w}$ and the nonlinear part \mathbf{N} . For both models we expand \mathbf{w} in orders of $\varepsilon^{1/2}$:

$$\mathbf{w} = \varepsilon^{1/2} \mathbf{w}_1 + \varepsilon \mathbf{w}_2 + \varepsilon^{3/2} \mathbf{w}_3 + O(\varepsilon^2), \quad (10)$$

leading to

$$\mathcal{L} = \mathcal{L}_0 + (\varepsilon \mathcal{L}_1 + \varepsilon^2 \mathcal{L}_2) \partial_X^2 + O(\varepsilon^3), \quad (11)$$

$$\mathbf{N} = \varepsilon \mathbf{N}_2 + \varepsilon^{3/2} \mathbf{N}_3 + \varepsilon^2 \mathbf{N}_4 + \varepsilon^{5/2} \mathbf{N}_5 + O(\varepsilon^3). \quad (12)$$

Inserting the new scalings and expansions into Eq. (9) requires a sorting of the basic equations up to two orders higher in $\varepsilon^{1/2}$ than for common spatial patterns [34]:

$$\varepsilon^{1/2} : \mathcal{L}_0 \mathbf{w}_1 = 0, \quad (13a)$$

$$\varepsilon : \mathcal{L}_0 \mathbf{w}_2 = -\mathbf{N}_2, \quad (13b)$$

$$\varepsilon^{3/2} : \mathcal{L}_0 \mathbf{w}_3 = -\mathcal{L}_1 \partial_X^2 \mathbf{w}_1 - \mathbf{N}_3, \quad (13c)$$

$$\varepsilon^2 : \mathcal{L}_0 \mathbf{w}_4 = \partial_{T_3} \mathbf{w}_1 - \mathcal{L}_1 \partial_X^2 \mathbf{w}_2 - \mathbf{N}_4, \quad (13d)$$

$$\varepsilon^{5/2} : \mathcal{L}_0 \mathbf{w}_5 = \partial_{T_3} \mathbf{w}_2 + \partial_T \mathbf{w}_1 - \mathcal{L}_1 \partial_X^2 \mathbf{w}_3 - \mathcal{L}_2 \partial_X^2 \mathbf{w}_1 - \mathbf{N}_5. \quad (13e)$$

For model *P*, we find at order $\varepsilon^{1/2}$ [41]

$$\mathbf{w}_1 = \tilde{A}(X, T) \begin{pmatrix} f_v \\ -f_u \end{pmatrix}. \quad (14)$$

Note that in contrast to the Ginzburg-Landau equation for stripes, $\tilde{A}(X, T)$ in our case is not the envelope of an underlying small-scale structure. An iterative solution of the hierarchy, Eqs. (13), leads to a dynamical equation for \tilde{A} via Fredholm alternatives at orders ε^2 and $\varepsilon^{5/2}$ [34]. After returning to the original coordinates x and t , and rescaling the amplitude $A = \sqrt{\varepsilon} \tilde{A}$, it takes the following form:

$$\partial_t A = -\partial_x^2 [\alpha_1 \varepsilon A + \alpha_2 \partial_x^2 A - \alpha_3 A^2 - \alpha_4 A^3]. \quad (15)$$

This is the Cahn-Hilliard model in one dimension [37] with a quadratic nonlinearity $\propto A^2$ (where $\alpha_1, \alpha_2, \alpha_4 > 0$). It corresponds to nonsymmetric mixtures of two liquids at thermal equilibrium. Equation (15) covers the approximate dispersion relation of the full model in Eq. (5) and nonlinearities up to third order in A . The derivation of the CH equation via the introduced reduction scheme automatically provides a mathematical link to the model for cell polarization in Eqs. (2). That is, the coefficients α_i are expressed by the parameters of the full model:

$$\alpha_1 = D_u f_v / b, \quad \alpha_2 = D_u^2 f_v / (b f_u), \quad (16a)$$

$$\alpha_3 = D_u b (3M - 1) / f_u, \quad \alpha_4 = D_u b^2 / f_u, \quad (16b)$$

with $f_u = -3M^2 + 2M - b$ and $f_v = -3M^2 + 2M$.

By application of the reduction scheme, the chemotaxis model *C* reduces to a similar equation for the density variation

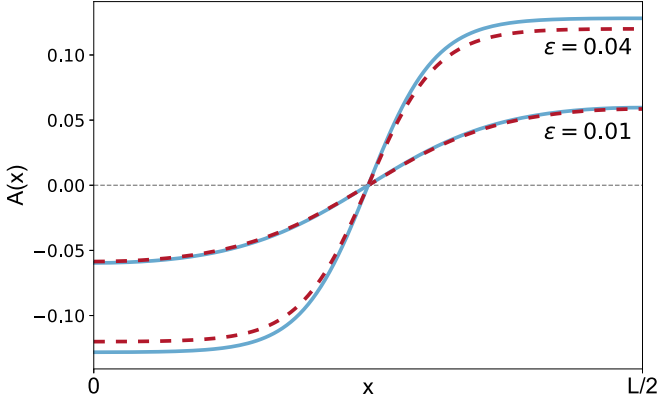


FIG. 1. Steady-state profiles $A(x)$ in the symmetric case ($M = 1/3$): Comparison of model P , Eqs. (2) (solid lines), to the corresponding solutions of the reduced CH model, Eq. (15) (dashed lines), for two values of the control parameter $\varepsilon = 0.01, 0.04$.

ρ , but with different coefficients [41]:

$$\partial_t \rho = -\partial_x^2 [\varepsilon \rho + D_c \partial_x^2 \rho + \frac{1}{2} s_c h^2 \rho^2 - \frac{1}{3} s_c \beta h^3 \rho^3]. \quad (17)$$

Note that the chemical signal c follows the cell density adiabatically.

The reduced models, Eqs. (15) and (17), capture the dynamics of the respective slow mode of phase separation [34]. Both CH models follow potential dynamics [38] even though the full Eqs. (2) and (4) do not. These qualities are a direct parallel to stripe patterns and their representation via the universal Ginzburg-Landau equation [30,34–36]. Thus, similar to the amplitude equation for stripes, we expect the CH model to play a generic role for active phase separation. Note that the reduced CH models, Eqs. (15) and (17), describe the behavior of a *conserved order parameter*—a reflection of the conservation constraints placed upon the original models P and C . The reduced models certainly cover the behavior of the full system near the (supercritical or weakly subcritical) bifurcation point. But in which parameter range further from the onset of phase separation does this agreement prevail? We will explore this by comparison of stationary solutions for the cell polarization model [cf. Eqs. (2)] and its approximation by the CH model in Eq. (15). We first study the special case $M = 1/3$, i.e., $\alpha_3 = 0$ and \pm symmetry of Eq. (15). This corresponds to the classic CH model [37]. For this case we compare in Fig. 1 steady-state solutions of the full model P to those of the related CH model for two different control parameter values ε (see Supplemental Material [41] for details on simulation methods). Due to the \pm symmetry in Eq. (15), the maximum and minimum of these profiles have the same absolute value. According to the conservation condition, the two phases with increased or decreased concentration each occupy half the system. With respect to both properties, the CH model covers the behavior of the full model. With increasing ε , the plateau values of the steady-state profiles increase and the coherence length decreases. Consequently, the profiles in Fig. 1 evolve toward a more steplike form. Note that in Figs. 1–5, the amplitude for the full model is calculated from the field v . The amplitude for u resembles the amplitude A from Eq. (15) even more closely.

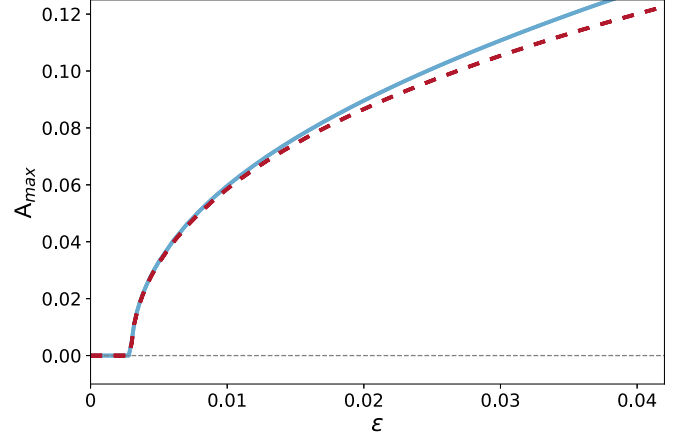


FIG. 2. Plateau values of the steady-state solutions in the symmetric case ($M = 1/3$): Comparison of model P , Eqs. (2) (solid line), to the corresponding values of the reduced CH model, Eq. (15) (dashed line), as a function of the control parameter ε .

Figure 2 shows the plateau values of the steady-state solutions as a function of ε . It thereby illustrates the validity range of the CH model—including the perfect agreement at onset, and the expected increasing deviations with increasing ε . Figure 2 also illustrates that the transition to active phase separation in the symmetric case occurs in a supercritical bifurcation. Note that the finite system size shifts the onset of phase separation to a positive value $\varepsilon_c = \alpha_2 \pi^2 / (L^2 \alpha_1)$ ($= 0.00296$ for the chosen parameters).

For $M \neq 1/3$, the quadratic term in Eq. (15) is finite. This leads to asymmetric phase separation, where the concentration deviates asymmetrically from its mean value. An example of this scenario is shown in Fig. 3 for $M = 0.3$. This corresponds to a small asymmetry parameter $\alpha_3 / \sqrt{\alpha_4} \simeq 0.055$. In this case, Eq. (15) captures the behavior of the full model very well. A comparison between the CH equation and the full model as a function of ε is presented in Fig. 4. In the presence of A^2 , the bifurcation from the homogeneous state

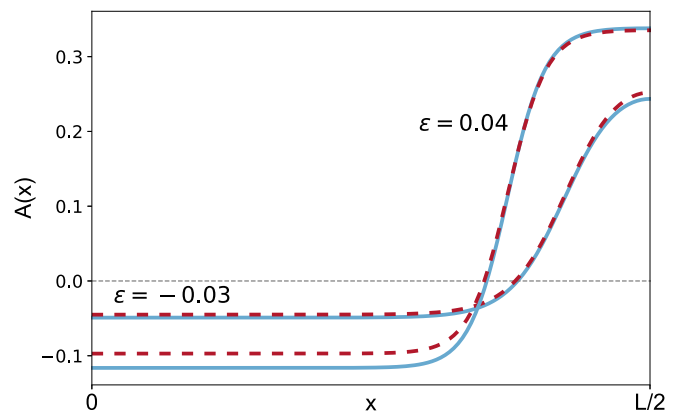


FIG. 3. Similar as in Fig. 1, but in the asymmetric case ($M = 0.3$), i.e., with the A^2 contribution in Eq. (15). Steady-state profiles of model P , Eqs. (2) (solid lines), compared to the corresponding solutions of the reduced CH model, Eq. (15) (dashed lines), for two values of the control parameter $\varepsilon = -0.03, 0.04$.

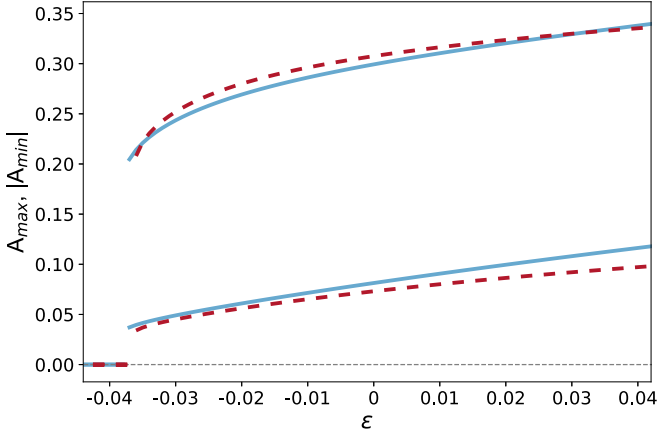


FIG. 4. Similar as in Fig. 2, but in the asymmetric case ($M = 0.3$). Upper and modulus of the lower plateau values of model P , Eqs. (2) (solid lines), compared to the corresponding values of the reduced CH model, Eq. (15) (dashed lines), as a function of the control parameter ε .

to phase separation is subcritical. That is, we find a jump from $A = 0$ to finite plateau values. Moreover, we observe the phase-separated state already for subcritical control parameter values. If the asymmetry parameter $\alpha_3/\sqrt{\alpha_4}$ is of $O(\sqrt{\varepsilon})$, both nonlinear terms in Eq. (15) are of the same order. As Fig. 5 shows, the reduced CH model is a good representation of the full model up to these moderate asymmetries. For stronger asymmetries, however, the full model may deviate strongly from its approximation [41]. That is, the full model may exhibit either for strong asymmetries or for large values of ε its own nongeneric “dialect” of active phase separation.

In this work, we identify a generic, system-spanning behavior for a number of very different demixing phenomena in active and living systems—a class of active phase separation. We have shown that this nonequilibrium transition is at leading order described by the CH equation [37,38]—the same equation that usually describes phase separation at thermal equilibrium. All models in this class have three central

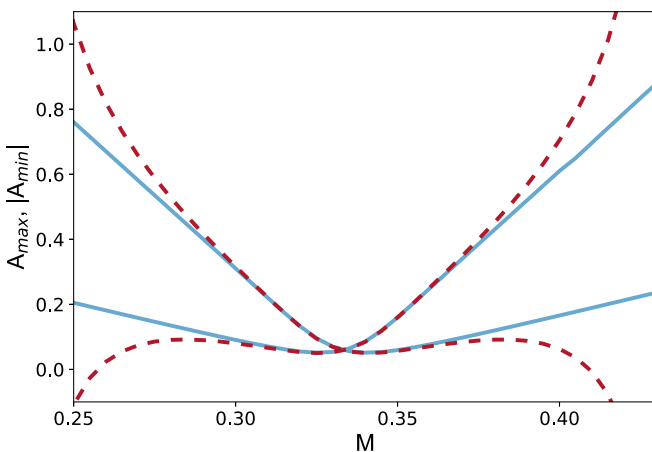


FIG. 5. Upper and modulus of the lower plateau values of the full (dashed lines) vs reduced model (solid lines) as a function of the asymmetry parameter M at a fixed control parameter value $\varepsilon = 0.01$.

properties in common: First, the slow mode growing out of a homogeneous basic state is conserved. Second, the slow mode follows the dispersion relation in Eq. (5). Third, nonlinearities up to third order in the order-parameter fields are sufficient near onset of active phase separation. These conditions ensure the correct signs of the coefficients α_i in the CH equation, Eq. (15). Furthermore, we introduced a perturbative reduction scheme that allows a direct derivation of the CH equation from system-specific nonequilibrium models. With this mathematical link, we can also determine the system-specific values of the coefficients in the CH model. This even allows for a quantitative comparison between the CH model and the original model equations. Note that the derived CH model follows potential dynamics [38], even though the system-specific equations—as the starting point of the reduction—are nonpotential systems.

We verified our generic approach by applying it explicitly to two active matter systems: a minimal model of cell polarization and a model for clustering in chemotactic cell communities. We found a convincing validity range of the generic CH equation as a representation of a cell polarization model near onset. Beyond the system-specific validity range of the CH model further interesting individual “dialects” of active phase separation may come into play. These include, for instance, the effects of higher-order nonlinearities covered by the full system-specific models. The so-called “active model B ,” for example, was recently introduced for modeling the nonequilibrium phenomenon “motility-induced phase separation” (MIPS) by a single mean field [42,43]. It includes the higher-order nonlinearity $\Delta[\nabla A(\mathbf{r})]^2 \propto \varepsilon^3$. This additional contribution renders the active model B nonintegrable [42] (see Supplemental Material [41] for a more detailed discussion of integrability with higher-order nonlinearities). However, this higher-order contribution becomes negligible near the onset of active phase separation, i.e., the validity range of the generic CH model. For some systems, fluctuations may also become relevant—especially for the coarsening dynamics in low spatial dimensions. This is similar to coarsening in equilibrium phase separation [38].

Our work also suggests the universality of phase separation processes—whether in or out of equilibrium. Their shared characteristics at leading order are reflected in the joint representation by the CH model. Our insights justify the recent usage of the CH equation as a phenomenological model for the clustering phenomenon observed for mussels [28] and further nonequilibrium demixing phenomena.

We expect our generic reduction to the CH model to work for further systems showing active phase separation. These include active colloids [18,21,43], active matter systems [22], or ion channels [27]. We anticipate these systems to also show the fingerprints of the class of active phase separation we introduced here for systems with a conserved order parameter. In this sense, our results are a conceptual parallel to the Ginzburg-Landau equation for an unconserved order parameter [30,34–36], which captures the essence of nonequilibrium stripe patterns near onset and also follows potential dynamics.

Our generic approach is a starting point for further investigations of nonequilibrium phenomena in systems with conserved quantities. Possible generalizations are order-parameter

models that also cover systems with more general dispersion relations than in Eq. (5) (see, e.g., Refs. [44,45]) or oscillatory phase separation phenomena.

Support by the Elite Study Program Biological Physics and inspiring exchanges with W. Pesch, I. Rehberg, and M. Weiss are gratefully acknowledged.

-
- [1] D. S. Johnston and J. Ahringer, *Cell* **141**, 757 (2010).
- [2] B. J. Thompson, *Development* **140**, 13 (2013).
- [3] N. W. Goehring and S. W. Grill, *Trends Cell Biol.* **23**, 72 (2013).
- [4] A. Jilkine, A. F. M. Marée, and L. Edelstein-Keshet, *Bull. Math. Biol.* **69**, 1943 (2007).
- [5] M. Otsuji, S. Ishihara, C. Co, K. Kaibuchi, A. Mochizuki, and S. Kuroda, *PLoS Comput. Biol.* **3**, e108 (2007).
- [6] Y. Mori, A. Jilkine, and L. Edelstein-Keshet, *Biophys. J.* **94**, 3684 (2008).
- [7] A. B. Goryachev and A. V. Pokhilko, *FEBS Lett.* **582**, 1437 (2008).
- [8] A. Jilkine and L. Edelstein-Keshet, *PLoS Comput. Biol.* **7**, e1001121 (2011).
- [9] B. Rubinstein, B. D. Slaughter, and R. Li, *Phys. Biol.* **9**, 045006 (2012).
- [10] P. K. Trong, E. M. Nicola, N. W. Goehring, K. V. Kumar, and S. W. Grill, *New J. Phys.* **16**, 065009 (2014).
- [11] S. Alonso and M. Bär, *Phys. Biol.* **7**, 046012 (2010).
- [12] N. W. Goehring, P. K. Trong, J. S. Bois, D. Chowdhury, E. M. Nicola, A. A. Hyman, and S. W. Grill, *Science* **334**, 1137 (2011).
- [13] E. F. Keller and L. A. Segel, *J. Theor. Biol.* **26**, 399 (1970).
- [14] E. F. Keller and L. A. Segel, *J. Theor. Biol.* **30**, 225 (1971).
- [15] M. J. Tindall, P. K. Maini, S. L. Porter, and J. P. Armitage, *Bull. Math. Biol.* **70**, 1570 (2008).
- [16] T. Hillen and K. J. Painter, *J. Math. Biol.* **58**, 183 (2009).
- [17] M. Meyer, L. Schimansky-Geier, and P. Romanczuk, *Phys. Rev. E* **89**, 022711 (2014).
- [18] J. Palacci, S. Sacanna, A. P. Steinberg, D. J. Pine, and P. M. Chaikin, *Science* **339**, 936 (2013).
- [19] I. Buttinoni, J. Bialké, F. Kümmel, H. Löwen, C. Bechinger, and T. Speck, *Phys. Rev. Lett.* **110**, 238301 (2013).
- [20] J. Stenhammar, A. Tiribocchi, R. J. Allen, D. Marenduzzo, and M. E. Cates, *Phys. Rev. Lett.* **111**, 145702 (2013).
- [21] T. Speck, J. Bialké, A. M. Menzel, and H. Löwen, *Phys. Rev. Lett.* **112**, 218304 (2014).
- [22] J. S. Bois, F. Jülicher, and S. W. Grill, *Phys. Rev. Lett.* **106**, 028103 (2011).
- [23] A. Y. Grosberg and J. F. Joanny, *Phys. Rev. E* **92**, 032118 (2015).
- [24] J. Stenhammar, R. Wittkowski, D. Marenduzzo, and M. E. Cates, *Phys. Rev. Lett.* **114**, 018301 (2015).
- [25] S. N. Weber, C. A. Weber, and E. Frey, *Phys. Rev. Lett.* **116**, 058301 (2016).
- [26] J. Smrek and K. Kremer, *Phys. Rev. Lett.* **118**, 098002 (2017).
- [27] P. Fromherz and B. Kaiser, *Europhys. Lett.* **15**, 313 (1991).
- [28] Q.-X. Liu, A. Doelman, V. Rottschäfer, M. de Jager, P. M. J. Herman, M. Rietkerk, and J. van de Koppel, *Proc. Natl. Acad. Sci. USA* **110**, 11905 (2013).
- [29] P. Ball, *The Self-Made Tapestry: Pattern Formation in Nature* (Oxford University Press, Oxford, 1998).
- [30] M. C. Cross and H. Greenside, *Pattern Formation and Dynamics in Nonequilibrium Systems* (Cambridge University Press, Cambridge, 2009).
- [31] S. Kondo and T. Miura, *Science* **329**, 1616 (2010).
- [32] E. Meron, *Nonlinear Physics of Ecosystems* (CRC Press, Boca Raton, FL, 2015).
- [33] I. Aranson and L. Kramer, *Rev. Mod. Phys.* **74**, 99 (2002).
- [34] M. C. Cross and P. C. Hohenberg, *Rev. Mod. Phys.* **65**, 851 (1993).
- [35] A. C. Newell and J. A. Whitehead, *J. Fluid Mech.* **38**, 279 (1969).
- [36] L. A. Segel, *J. Fluid Mech.* **38**, 203 (1969).
- [37] J. W. Cahn and J. E. Hilliard, *J. Chem. Phys.* **28**, 258 (1958).
- [38] A. J. Bray, *Adv. Phys.* **43**, 357 (1994).
- [39] L. Wolpert, *Principles of Development* (Oxford University Press, Oxford, 2002).
- [40] The introduction of two timescales is a mathematical necessity to solve the following hierarchy of Eqs. (13). There the solvability condition in the order ε^2 demands the introduction of an additional timescale T_3 . In the final Eqs. (15) and (17), this timescale leads to the additional quadratic term compared to the classical Cahn-Hilliard model.
- [41] See Supplemental Material at <http://link.aps.org/supplemental/10.1103/PhysRevE.98.020603> for more detailed calculations, simulation methods, and discussions about strong asymmetries and higher-order nonlinearities.
- [42] R. Wittkowski, A. Tiribocchi, J. Stenhammar, R. J. Allen, D. Marenduzzo, and M. E. Cates, *Nat. Commun.* **5**, 4351 (2013).
- [43] M. E. Cates and J. Tailleur, *Annu. Rev. Condens. Matter Phys.* **6**, 219 (2015).
- [44] S. M. Murray and V. Sourjik, *Nat. Phys.* **13**, 1006 (2017).
- [45] F. Meng, D. Matsunaga, and R. Golestanian, *Phys. Rev. Lett.* **120**, 188101 (2018).